MAX-PLANCK-INSTITUT FÜR PLASMAPHYSIK

GARCHING BEI MÜNCHEN

ABSORPTION OF THE LOWER-HYBRID WAVE IN A THERMONUCLEAR PLASMA

S. Puri

IPP IV/76 August 1974

Die nachstehende Arbeit wurde im Rahmen des Vertrages zwischen dem Max-Planck-Institut für Plasmaphysik und der Europäischen Atomgemeinschaft über die Zusammenarbeit auf dem Gebiete der Plasmaphysik durchgeführt.

IPP IV/76 S. Puri

Absorption of the Lower-Hybrid Wave in a Thermonuclear Plasma ++)

August 1974 (in English)

Abstract

Computations using the full hot-plasma dielectric tensor show that the lower-hybrid characteristics depart significantly from the analytic results of Stix[1] and Glagolev[2]. The discrepancy is traced to the neglect of the terms involving higher-order Bessel functions while performing the summations for obtaining the components of the dielectric tensor, leading to the breakdown of the analytical approaches in the neighbourhood of the resonance. For typical thermonuclear parameters the damping term due to electron resistivity dwarfs the contribution due to Landau damping. Unlike the conclusions of Refs. 1 and 2, conversion of the lower-hybrid wave to either the acoustic or the cyclotron-harmonic modes seems neither plausible nor necessary for the purpose of energy absorption.

Boundary value solutions using stepped slab model show that the penetration problem of the electromagnetic wave into the plasma is not materially affected by the inclusion of finite temperature effects. As the wave approaches the hybrid layer, the Poynting vector decreases with a corresponding increase in the energy transport due to the particle motion. This energy is, in turn, deposited into the plasma electrons through resistive absorption near the resonant layer where the group velocity becomes considerably less than the ion-thermal speed. The wave is efficiently absorbed even at the plasma temperature of 10^8 ^oK when the ratio of collision frequency to wave frequency, $\nu/\omega \sim 10^{-7}$.

++) Invited paper to be presented in the symposium on "Plasma Heating in Toroidal Devices", Varenna, 3 - 17 September 1974.

ABSORPTION OF THE LOWER-HYBRID WAVE IN A THERMONUCLEAR PLASMA

S. Puri
Max-Planck-Institut für Plasmaphysik, D-8046 Garching

ABSTRACT

Computations using the full hot-plasma dielectric tensor show that the lower-hybrid characteristics depart significantly from the analytic results of Stix[1] and Glagolev[2]. The discrepancy is traced to the neglect of the terms involving higher-order Bessel functions while performing the summations for obtaining the components of the dielectric tensor, leading to the breakdown of the analytical approaches in the neighbourhood of the resonance. For typical thermonuclear parameters the damping term due to electron resistivity dwarfs the contribution due to Landau damping. Unlike the conclusions of Refs. 1 and 2, conversion of the lower-hybrid wave to either the acoustic or the cyclotron-harmonic modes seems neither plausible nor necessary for the purpose of energy absorption.

Boundary value solutions using stepped slab model show that the penetration problem of the electromagnetic wave into the plasma is not materially affected by the inclusion of finite temperature effects. As the wave approaches the hybrid layer, the Poynting vector decreases with a corresponding increase in the energy transport due to the particle motion. This energy is, in turn, deposited into the plasma electrons through resistive absorption near the resonant layer where the group velocity becomes considerably less than the ion-thermal speed. The wave is efficiently absorbed even at the plasma temperature of 10^8 ^oK when the ratio of collision frequency to wave frequency, $\nu/\omega \sim 10^{-7}$.

THE DISPERSION CHARACTERISTICS

Ever since the derivation of the hot-plasma dielectric tensor in an explicit form by Stepanov[3] in 1958, it has been possible, in principle, to compute the dispersion characteristics of linear waves in magnetized, hot, homogeneous plasmas. Such an effort would be rewarding for evaluating the possibility of radio-frequency ignition of thermonuclear plasmas. It is a reflection on the complexity of the undertaking that barring the cases of propagation strictly parallel (Landau waves) and perpendicular (Bernstein modes) to the static magnetic field B_o, little accurate information of the wave behaviour is available.

In this paper we study (with an accuracy exceeding one part in a million) the finite temperature effects on the obliquely propagating shear (slow) and compressional (fast) cold-plasma modes using the complete hot-plasma dielectric tensor. The plasma density is allowed to have a gradient perpendicular to B_o (see Fig. 1). The scale of the gradient is left unspecified such that the "local" dielectric tensor approximation is valid. Anticipating the boundary conditions to be used in the next section, we shall employ the Derfler-Omura[4] dielectric tensor described in Eqs. (5 - 20) of Ref. 5. Since in the derivation of the Derfler-Omura tensor, the total plasma current is subdivided into the polarization and the magnetization currents, the tangential magnetic field at a boundary is continuous. In every other respect, this tensor is identical to the Stepanov tensor.

Electron resistivity contribution $\Delta\epsilon$ to the dielectric tensor ϵ is incorporated using the method described in Ref. 6,

$$\Delta\epsilon = i(\omega\,\nu_{ei}/\omega_{pe}^2)\quad(\epsilon - 1)\quad\cdot\quad(\epsilon - 1)$$

where ν_{ei} is the electron-ion momentum transfer collision frequency according to Spitzer[7] (the values of ν_{ei} quoted in this paper are for the average density of $3 \times 10^{13}\,\mathrm{cm}^{-3}$). This method of obtaining $\Delta\epsilon$ is admittedly crude. However, the dispersion curves are insensitive to the precise value of ν_{ei} and the error introduced will not alter the results in a significant manner.

Throughout this paper it is assumed that the ions (deuterium) and the electrons possess a maxwellian velocity distributions of equal temperatures. The static magnetic field B_o and the gradient of density are along the z and x-directions respectively. All field quantities are assumed to possess space and time dependence exp i $(k_x x + k_z z - \omega t)$ with no variation in the y-direction[8]. The dispersion equation then takes the form

$$a\,n_x^4 + b\,n_x^2 + c = o \qquad (1)$$

where,

$$a = \epsilon_{xx}\,\mu_{xx}$$

$$b = n_z^2\,(\epsilon_{xx}\,\mu_{zz} + \epsilon_{zz}\,\mu_{xx})$$
$$- \epsilon_{xx}\,\epsilon_{zz}\,(\mu_{xx}^2 + \mu_{xy}^2) - \mu_{xx}\,\mu_{zz}\,(\epsilon_{xx}^2 + \epsilon_{xy}^2)$$

$$c = \epsilon_{zz}\,\mu_{zz}\left[n_z^4 + 2\,n_z^2\,(\epsilon_{xy}\,\mu_{xy} - \epsilon_{xx}\,\mu_{xx}) + (\epsilon_{xx}^2 + \epsilon_{xy}^2)\;(\mu_{xx}^2 + \mu_{xy}^2)\right]$$

$n_x = c\,k_x/\omega$, $n_z = c\,k_z/\omega$ while ϵ and μ are defined in Ref. 5.

We shall restrict our attention to the roots of Eq. (1) identified as the shear (slow) and the compressional (fast) modes in the cold-plasma limit. For finite values of n_z, these cold-plasma modes exhibit propagation on the low-density side of the lower-hybrid resonance except near the plasma edge where evanescent or complex waves might exist. On the high density side of the resonance, the fast mode continues to propagate while the slow mode becomes evanescent. Introduction of electron resistivity modifies this behaviour somewhat and the resultant cold-plasma characteristics resemble the curves of Fig. 2b which are in fact obtained by solving Eq. (1) numerically for the case $T_e = T_i = 1$ eV.

Observe that the slow mode is a backward wave (recognized by the opposite signs of the real and imaginary parts of k_x) which transforms into a forward wave upon passing through the cutoff on the high-density side of the resonance. For temperatures below 10eV, the collisional effects dominate because the wavelength is much too long ($|k_x\, r_{ci}| \ll 1$) for the Larmor radius to play any prominent role. Marked changes, however, are seen to occur at higher temperatures ($T \gtrsim 100$ eV) when the Larmor radius becomes comparable with the wavelength. As might be expected the resonance is flattened and broadened occuring somewhat in advance of the hybrid density. Simultaneously an increased reluctance on the part of the slow wave to change its backward character is observed and beyond $T \sim 100$ eV, the cutoff disappears altogether resulting in a significantly altered dispersion characteristic of Fig. 2e ($T = 1$ keV). This trend continues up to the thermonuclear ignition temperature of 10 keV (Fig. 2f) and ear the resonance, the hot-plasma effects have altered the appearance of the curves beyond any recognition based on the cold-plasma theory.

Before entering into discussion of possible physical effects we make two observations pertinent to the problem of plasma heating at the lower hybrid resonance. Note that since $|k_x r_{ci}| \ll 1$ near the plasma edge irrespective of the temperature, it is justified to treat the problem of wave accessibility within the framework of the cold-plasma theory[9]. Also, even at thermonuclear temperatures $\mathrm{Im}(k_x^s)$ is large enough to allow complete absorption of the wave energy within a few Larmor radii.

Near the hybrid resonance $n_x \gg 1$, the dispersion characteristics (Fig. 1) are dominated by the dielectric tensor component ϵ_{xx} (since $\mu_{xx} \sim 1$) as can be seen in Fig. 3. At low temperatures $\mathrm{Re}\ \epsilon_{xx}$ (solid curve) goes through zero at the hybrid layer (cross on the density axis) while the collisions give rise to a small but finite $\mathrm{Im}\ \epsilon_{xx}$. n_x then acquires a finite imaginary part even ahead of the hybrid layer. Unlike the cold-plasma dispersion, in a hot plasma, $\mathrm{Im}\ n_x$ reacts back on ϵ_{xx} and the bootstrap effect causes a large increase in their imaginary parts at the same time significantly altering the real parts as well. This mathematical subtlety is mirrored in the physics as a reduction in the group velocity (Fig. 4) well ahead of the hybrid layer.

This obliges one to include collisions as an important fundamental effect in the understanding of the lower-hybrid propagation in a hot plasma. We shall presently see that the wave energy is efficiently absorbed by collisions right up to the thermonuclear temperatures. It is then not necessary to invoke additional dissipative mechanisms i.e. wave conversion, parametric or non-linear effects in order to obtain the necessary damping effects. The existing wave-conversion theories[1,2] assume the reflection of the lower-hybrid wave near the resonant layer and its subsequent transformation into the cyclotron and acoustic modes. Since the parent mechanism of wave reflection might be missing altogether, the prospects of wave-conversion are considerably diminished.

BOUNDARY VALUE SOLUTION

Central to the concept of boundary value problems in a hot plasma are

i) the notion of a boundary

and ii) the number and the nature of the boundary conditions.

It is apparent that if the wavelength we are dealing with is much larger than the particle excursions (e.g. the cyclotron radius), a localization of the particle orbit would be justifiable. This is, in fact, the cold-plasma assumption. In this case it would be sufficient to treat the plasma in the local approximation at intervals such that there is no significant alteration in either the propagation vector or the components of the dielectric constant. A more stringent condition would be to use the local approximation at intervals much smaller than the local value of the wavelength. Note that no stipulation is needed regarding the magnitude of the gradient itself.

More complex considerations prevail when the wavelength begins to approach the size of the particle orbits. The steepness of the gradient must be restricted so that no appreciable change in the parameters occurs for several Larmor radii for the validity of the "local" approximation. How many? A look at the normal distribution curve would show that in thermodynamical equilibrium no more than 0.1% of the particles would ever venture beyond two Larmor radii. Considering that an alteration in the dielectric constant is, furthermore, a differential effect, the gradient length exceeding two Larmor radii would provide us with acceptable practical answers.

If we assume that the ion-cyclotron modes propagate only to the right of the hybrid-layer, then for sufficiently large n_z there are only two known propagating (except for a negligibly narrow evanescent region) waves namely the slow and fast cold-plasma modes between the plasma edge and the hybrid layer. It would suffice to use the continuity of the $\underline{E}$ and $\underline{H}$ fields to solve the problem uniquely provided we assume for the present that there is no wave conversion. The reasonableness of this assumption has already been discussed in the last section.

The actual solution of the boundary value problem was carried out using a stepped slab model with one hundred plasma slabs. Note that once the physical assumptions are satisfied the computation accuracy increases with the number of slabs. A unit incident TM wave with n_z = .99 is partly reflected as a pair of TM and TE waves while the rest is transmitted into the plasma as the slow and fast modes. The fast mode propagates without much distinction whereas the slow mode field increases as the hybrid layer is approached (Fig. 5) when the dissipative effects dampen the wave. At the low or high temperatures the collisional dissipation appears early, before the amplification has a chance to create very high electric fields. Thereafter the two processes act simultaneously resulting in a broad region of energy deposition. At intermediate temperatures, on the other hand, the two processes are spatially exclusive resulting in an enormous accumulation of the wave energy followed by a very sudden decay. For plasma temperatures of thermonuclear interest (1 - 10 keV), the electric field buildup for forseeable energy fluxes is mild and any notion of non-linear effects can be comfortably set aside. Fortunately, too, the energy absorption occurs in a relatively wide region and, hence, hopefully diminished possibilities of catastrophic effects of rf heating on the plasma containment.

The last figure (Fig. 6) showing the spatial variation of the Poynting vector implies either absorption or a transfer of a part of the electromagnetic field energy to kinematic energy. This transfer process occurs in the steep parts of these curves at higher temperatures as has been confirmed by the separate and independent calculation of the kinematic energy flux. An interesting feature is the backstreaming and reconversion of this kinematic flux resulting in the peculiar peaks (see Fig. 6f) in the Poynting vector plots just before the rapid descent. At these peaks the Poynting vector exceeds the power coupled into the plasma at the vacuum boundary. We shall restrain the temptation to present the results of kinematic flux calculations due to their dubious validity in the presence of more than a single wave in the plasma. Observe that the wave accessibility is not appreciably affected by the change in plasma temperature. The problem of accessibility will be taken up in much greater detail in a future communication.

ACKNOWLEDGEMENT

This work has been done in a still continuing collaboration with Dr.M.Tutter I am indebted to Dr. P. Barberio-Corsetti for providing us with the program[10] for computing the plasma dispersion function. The author has benefited from discussions as well as stray remarks by Dr. F. Leuterer. Dr. H. Derfler was kind enough to draw our attention to the Derfler-Omura dielectric tensor.

This work has been performed as part of the joint research program between Euratom and the Max-Planck-Institut für Plasmaphysik.

REFERENCES

1 T.H. Stix, Phys. Rev. Lett. 15, 878 (1965).

2 V.M. Glagolev, Plasma Phys. 14, 315 (1972).

3 K.N. Stepanov, Sov. Phys. JETP 7, 892 (1958); Zh. Eksp. Teoret. Fiz. 34, 1292 (1958).

4 M. Omura, Electrostatic waves in Bounded Hot Plasmas, Stanford University IPR Report No. 156 (1967).

5 S. Puri, F. Leuterer, and M. Tutter, J. Plasma Phys. 9, 89 (1973); $\sqrt{2}$ in the RHS of Eq. (17) is superfluous while the RHS of Eq. (19) should be divided by 2. Both these errors are typographical.

6 T.H. Stix, Theory of Plasma Waves, McGraw Hill, New York (1962), p. 252.

7 L. Spitzer, Jr., Physics of Fully Ionized Gases, Interscience Publishers, New York (1962).

8 Since in Ref. 3 the signs of space and time dependence are reversed, the signs of ϵ_{xy} and μ_{xy} should be changed accordingly. Also the integration of z in Eq. (20) should be performed in the region Im $\zeta < 0$.

9 S. Puri, and M. Tutter, Nuclear Fusion 14, 93 (1974); also further references on this topic are listed here.

10 P. Barberio-Corsetti, Calculations of Plasma Dispersion Function, Princeton University Report MATT-773 (1970).

FIGURE CAPTIONS

Fig. 1 The geometry of the boundary value problem.

Fig. 2 Real (solid curves) and imaginary (partially dashed curves) parts of k_x versus density for both the fast and slow waves as a function of temperature. The pair of curves for the slow mode are readily recognized by the resonance characteristics near the lower-hybrid density (shown by a cross on the density axis). The straight dashed lines in (d-f) correspond to the location of the reciprocal ion-Larmor radius ($|k_x \ r_{ci}| = 1$). For all these curves $n_z = 0.99$, $\omega_{lh}/\omega_{ci} = 13.25$ and $B_o = 100$ kG. (The abrupt vertical crossings of the axis are due to the vertical scale being compressed quadratically to facilitate the representation near the axis).

Fig. 3 ϵ_{xx} versus density.

Fig. 4 Group velocity of the fast and the slow modes as a function of density. The validity (Im k $\ll$ Re k) of the group velocity concept is restricted to the region between the two top arrows for the fast mode and the two bottom arrows for the slow mode. For the slow mode this region does not exist for the case T = .1 eV. The cross on the density axis is the location of the lower-hybrid density while on the vertical axis represents the ion-thermal speed. The detail near the axis is exaggerated by the cubic compression of the vertical axis.

Fig. 5 Electric field component E_x in the plasma as a function of distance from the vacuum interface for the slow (solid curves) and the fast waves. The incident TM wave amplitude is assumed to be 1 volt/cm. In Fig. 5c the electric field peaks reach up to + 43 and down to - 22 volts. The coupling of the fast and the slow wave fields, when the imaginary part of the complex-conjugate propagation region near the plasma edge vanishes, is clearly visible. The more sharply pointed peak in Fig. 5e results from the precise coincidence of one of the slabs at the location where Im k_x is very nearly zero. Both the total energy coupled, as well as the partial energies of the slow and the fast waves are insensitive to this display of field coupling as is demonstrated by the scant change in these quantities as the positions of the slabs are shuffled.

Fig. 6 Poynting vector component P_x versus distance. The energy remaining in the wave after the hybrid layer represents the energy coupled into the fast wave. It is seen that over 70% of the total energy is coupled into the slow mode.

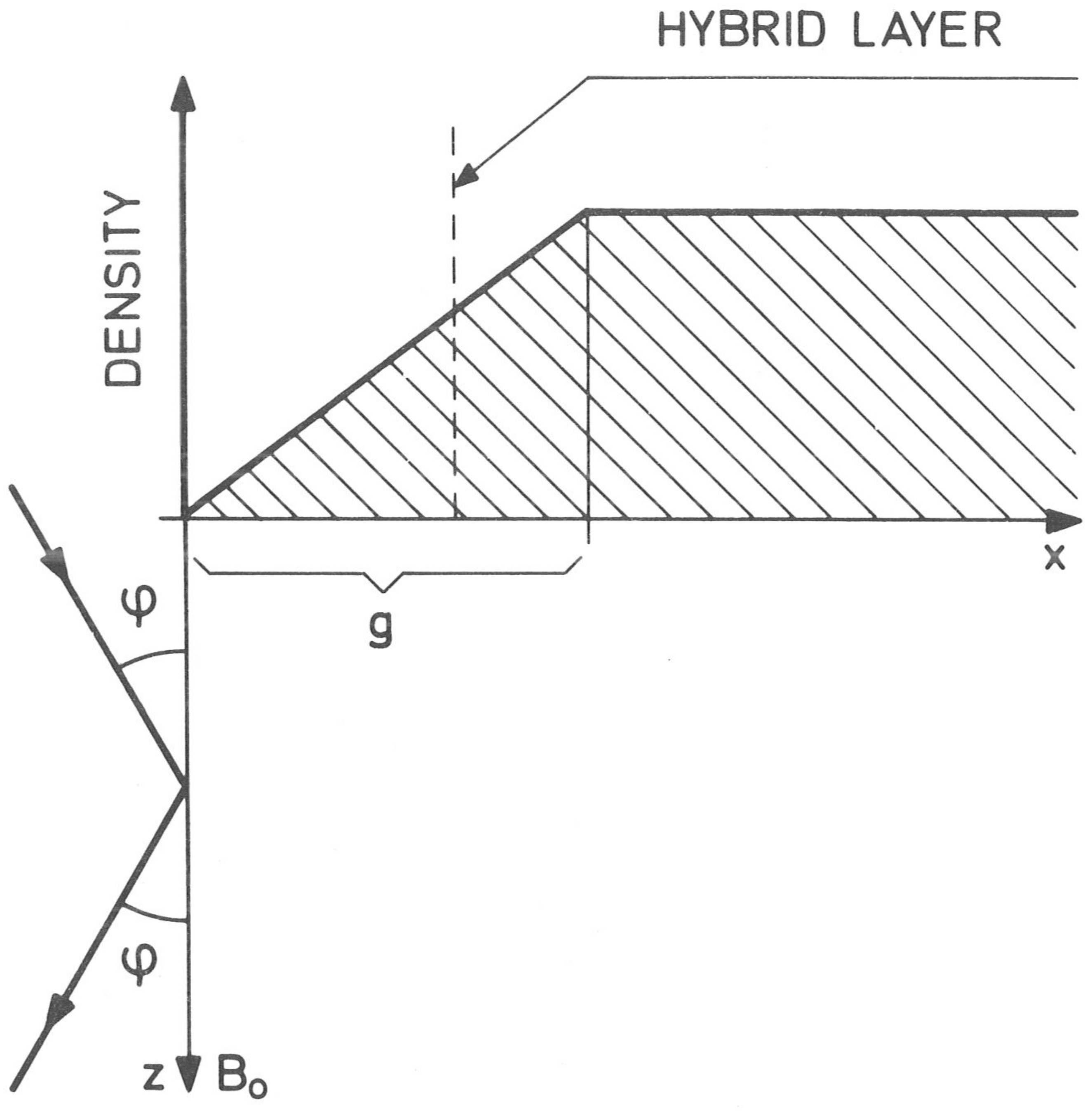

Fig. 1

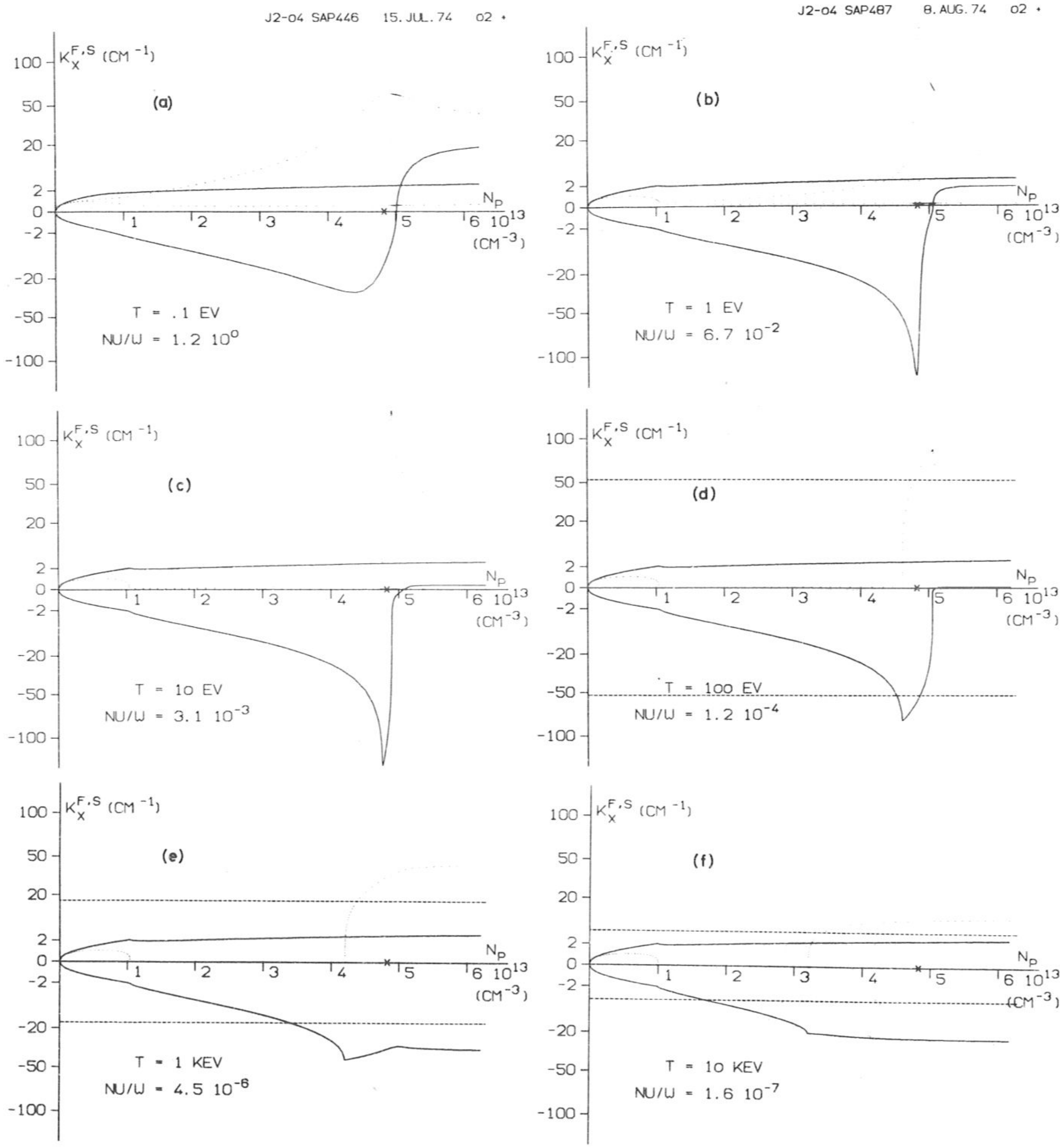
J2-04 SAP446 15. JUL. 74 02
J2-04 SAP487 8. AUG. 74 02
$K_X^{F,S}$ (CM $^{-1}$)
(a)
(b)
(c)
(d)
(e)
(f)
N_P
10^{13} (CM^{-3})
T = .1 EV
NU/W = 1.2 10^{0}
T = 1 EV
NU/W = 6.7 10^{-2}
T = 10 EV
NU/W = 3.1 10^{-3}
T = 100 EV
NU/W = 1.2 10^{-4}
T = 1 KEV
NU/W = 4.5 10^{-6}
T = 10 KEV
NU/W = 1.6 10^{-7}

Fig.2

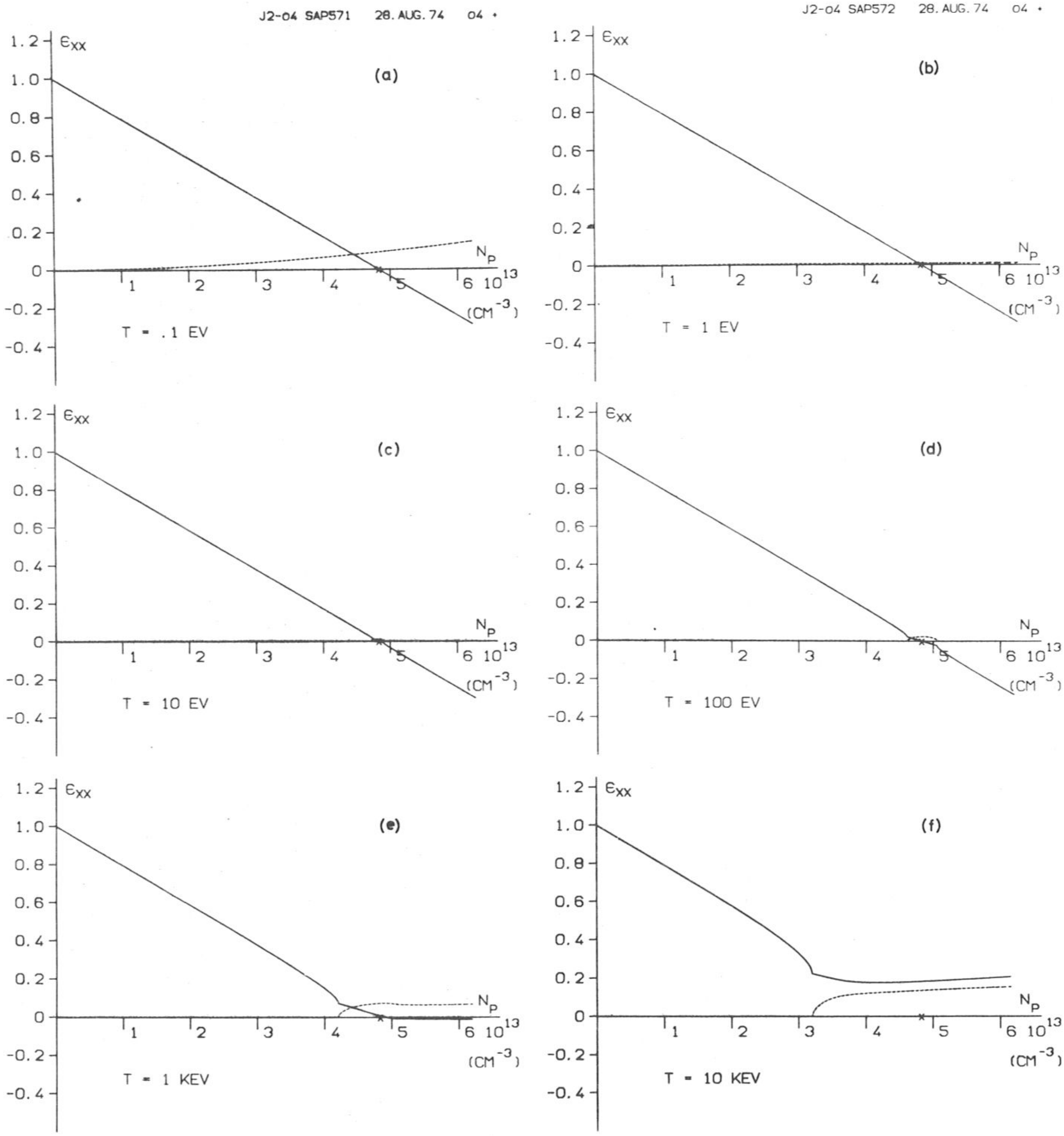

J2-04 SAP571 28. AUG. 74 04
J2-04 SAP572 28. AUG. 74 04
(a)
(b)
(c)
(d)
(e)
(f)
ϵ_{xx}
N_P
$6\ 10^{13}$
(CM^{-3})
1.2
1.0
0.8
0.6
0.4
0.2
0
-0.2
-0.4
1
2
3
4
5
T = .1 EV
T = 1 EV
T = 10 EV
T = 100 EV
T = 1 KEV
T = 10 KEV

Fig.3

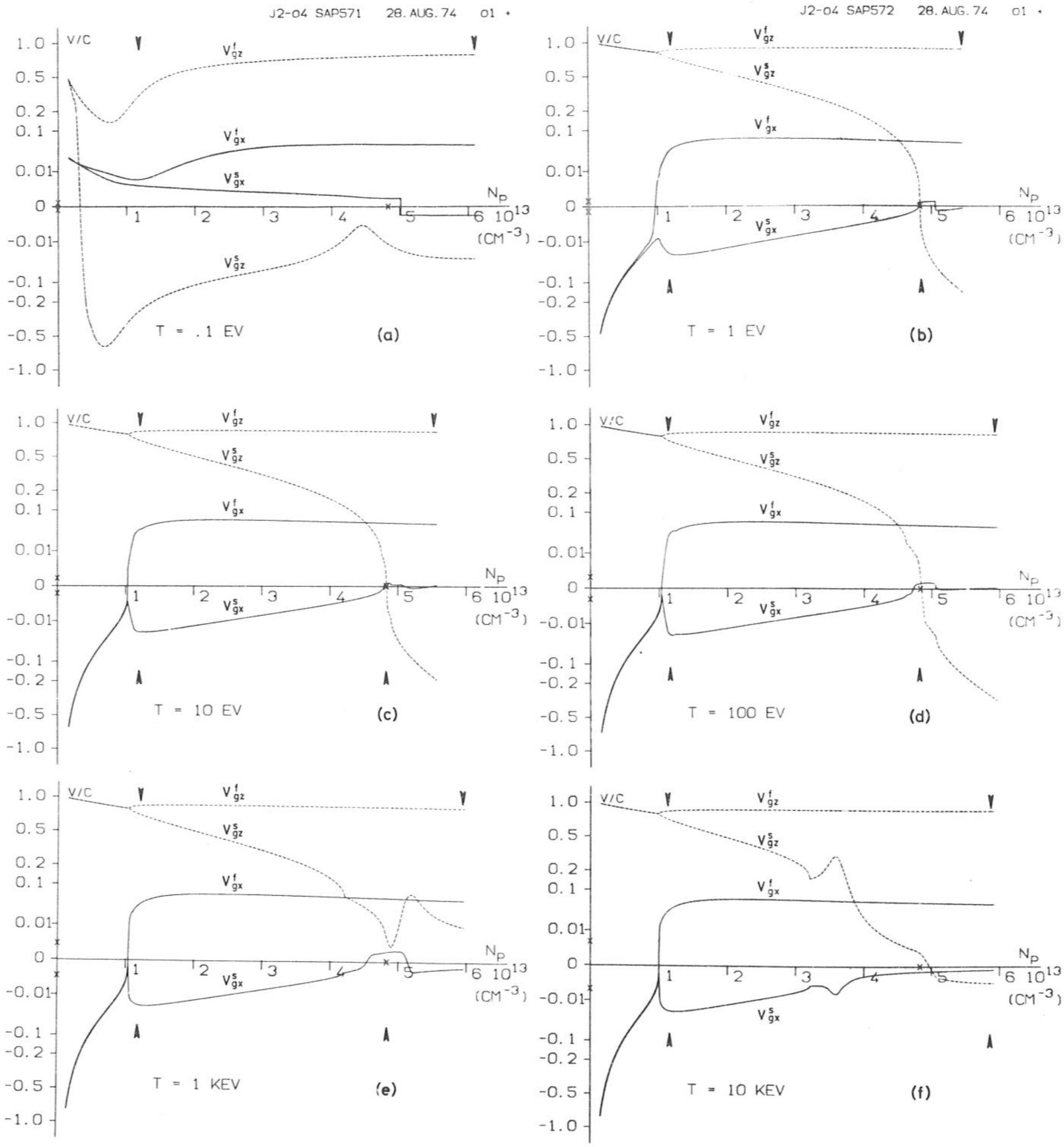
J2-04 SAP571 28. AUG. 74 01
J2-04 SAP572 28. AUG. 74 01
V/C
V_{gz}^f
V_{gz}^s
V_{gx}^f
V_{gx}^s
N_P
10^{13}
(CM^{-3})
T = .1 EV
(a)
T = 1 EV
(b)
T = 10 EV
(c)
T = 100 EV
(d)
T = 1 KEV
(e)
T = 10 KEV
(f)

Fig. 4

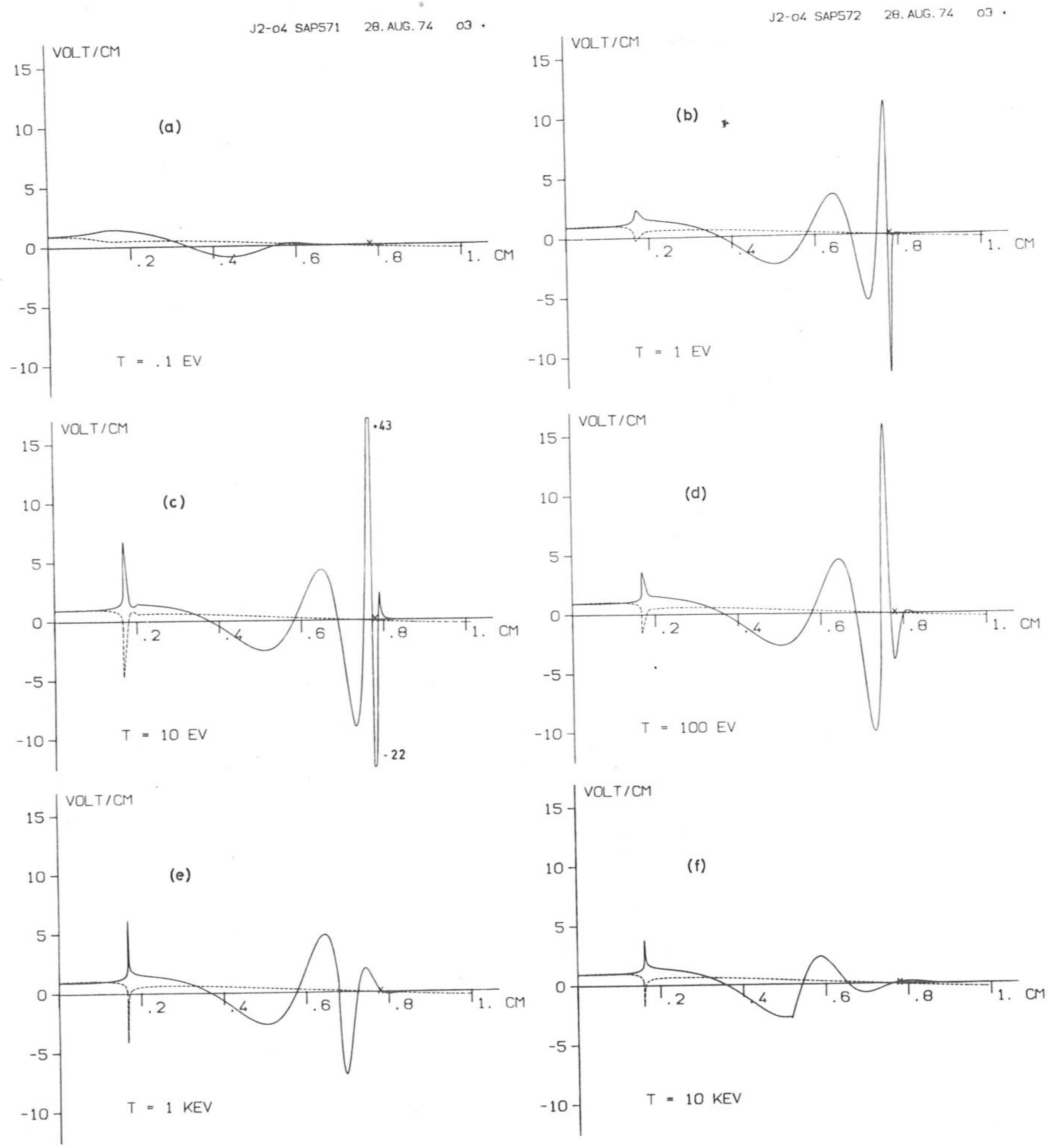
J2-04 SAP571 28. AUG. 74 03
J2-04 SAP572 28. AUG. 74 03
VOLT/CM
(a)
T = .1 EV
(b)
T = 1 EV
(c)
T = 10 EV
+43
-22
(d)
T = 100 EV
(e)
T = 1 KEV
(f)
T = 10 KEV
CM

Fig.5

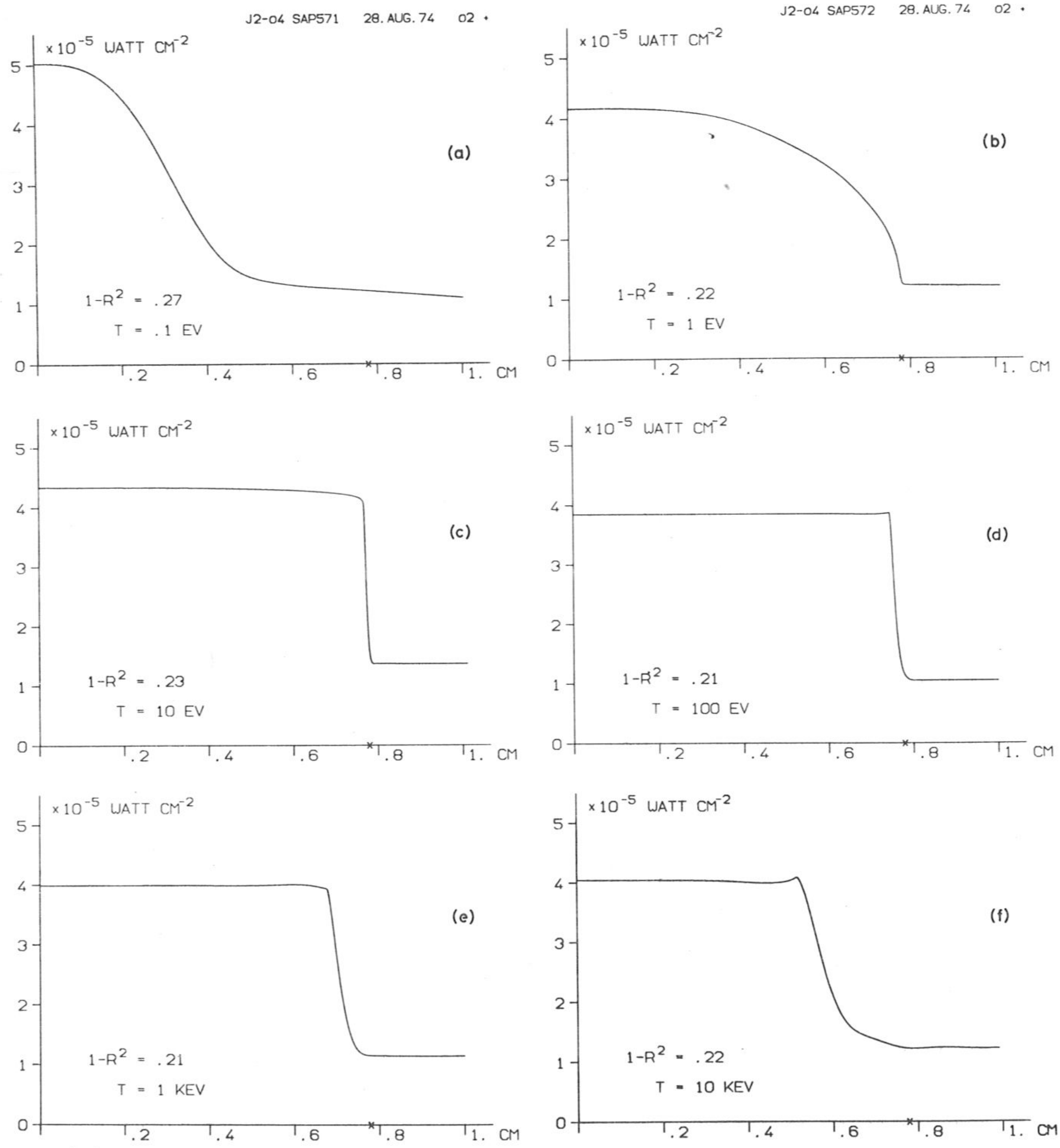
J2-04 SAP571 28. AUG. 74 02
J2-04 SAP572 28. AUG. 74 02
x 10^-5 WATT CM^-2
(a)
1-R^2 = .27
T = .1 EV
(b)
1-R^2 = .22
T = 1 EV
(c)
1-R^2 = .23
T = 10 EV
(d)
1-R^2 = .21
T = 100 EV
(e)
1-R^2 = .21
T = 1 KEV
(f)
1-R^2 = .22
T = 10 KEV
CM

Fig. 6